Comparison between Lagrangian and Eulerian methods for the simulation of particle-laden flows subject to radiative heating

By A. Vié, H. Pouransari, R. Zamansky† AND A. Mani

1. Motivation and objectives

Turbulent particle- or droplet-laden flows play a key role in numerous applications, including natural processes such as droplet clouds, dust storms, and protoplanetary disks, as well as in industrial applications such as fuel sprays in internal combustion engines, fluidized beds, particle-based solar receivers, and pharmaceutical sprays. Understanding the key processes underlying the coupled dynamics of particles and fluids in such systems requires the development of models capable of reproducing their physics. In most of these systems the particle-laden mixture is under turbulent conditions, and turbulence can induce preferential concentration in the particle field (Squires & Eaton 1991*b*; Elgobashi & Truesdell 1992; Eaton & Fessler 1994; Fessler *et al.* 1994): inertial particles are ejected from vortex cores and accumulated in low-vorticity zones. This phenomenon is characterized by the particle Stokes number $St_k = \tau_p/\tau_k$, i.e., the ratio between the particle inertial relaxation time to the Kolmogorov time scale of the turbulence (Eaton & Fessler 1994).

Previous investigations have indicated that preferential concentration is strongest for systems with a Stokes number of order unity (Eaton & Fessler 1994). Very small particles with small Stokes number essentially follow the flow streamlines, and cannot be effectively centrifuged outside of vortex zones; in the limit of very large Stokes number, the particle phase is hardly influenced by the flow field and thus the effects of preferential concentration are suppressed. Preferential concentration plays a key role in various processes including enhancement of particle-particle collision (e.g., leading to faster particle agglomeration or drop coalescence Sundaram & Collins (1997); Wang *et al.* (1998)), and turbulence modulation (Gore & Crowe 1989; Elgobashi & Truesdell 1993; Fessler *et al.* 1994; Boivin *et al.* 1998). In some scenarios preferential concentration plays a primary role even in generating and sustaining turbulence (Zamansky *et al.* 2014; Mizukami *et al.* 1992). Therefore, when it comes to modeling of particle-laden flow phenomena, one key concern is the capability of the model to capture preferential concentration.

Early numerical models attempted to couple Lagrangian particle methods with traditional Eulerian fluid turbulence simulations (Riley & Patterson 1974; Elgobashi & Truesdell 1992; Squires & Eaton 1991*a,b*). In the most simple limit, trajectory of the particles can be determined by use of the Stokes drag formula (Stokes 1851). In this study, the following assumptions are made: (i) the particles are smaller than the Kolmogorov length scale ($d < \eta$), microscopic particle-resolved DNS is not necessary, and a mesoscopic‡ point-particle approximation is envisaged (Maxey & Riley 1983; Fox 2012);

‡ Microscopic details of the flow field around the particle are embedded into a mesoscopic closure like Stokes drag.

(ii) the density between the particles and the gas phase is large ($\rho_p >> \rho_g$), so that the drag force is the dominant external force that is acting on the particle motion; (iii) the Reynolds number of the particles is smaller than one ($\text{Re}_p < 1$), the Stokes drag formulation can be used, i.e., the relaxation time of the particle is $\tau_p = \rho_p d^2 / 18\mu_g$, where ρ, μ, and d denote density, viscosity, and particle diameter respectively, and subscripts p and g represent particle and fluid (gas), respectively; (iv) a dilute regime is considered, thus the volume fraction is small ($\alpha_p < 10^{-3}$) enough so that particle-particle collision would have a negligible impact on primary dynamics; (v) the mass loading is small ($\alpha_p \rho_p / \rho_g < 10^{-2}$), so momentum two-way coupling between the two phases is avoided; (vi) the particles are solid and spherical, so the size of the particles does not change with time; (vii) and the particles have a negligible heat capacity ($c_{p,particle} << c_p$), so that the heat absorbed by the particles is immediately transferred to the gas phase and there is no need to solve the temperature equation of the particle.

Under such conditions, Lagrangian point particle methods have been tested against experiments and were shown to be able to capture the preferential concentration phenomena fairly accurately (Squires & Eaton 1991*a*; Elgobashi & Truesdell 1992). In a typical simulation, the number of numerical particles would be equal to the number of physical particles. Following these simplifications, the equations for the Lagrangian particles are limited to their position $\mathbf{X}_p$ and velocity $\mathbf{U}_p$

$$\frac{\mathrm{d}\mathbf{X_P}}{\mathrm{d}t} = \mathbf{V_P}, \tag{1.1}$$

$$\frac{\mathrm{d}\mathbf{V_P}}{\mathrm{d}t} = \frac{\mathbf{u_g}(t, \mathbf{X_P}) - \mathbf{V_P}}{\tau_p}, \tag{1.2}$$

where $\tau_p = \frac{\rho_p d^2}{18\mu_g}$ is the relaxation time of the particles and u_g the gas phase velocity.

In the context of mesoscopic DNS simulations, the Lagrangian particle tracking is the reference. However, it still has some limitations. First, if one is aiming at the statistics of the disperse phase, i.e., the values of local Number Density Function (NDF), many realizations are needed to develop converged statistics. Additionally, when the average number of particles per control volume is large, Lagrangian methods can become very expensive due to the extensive computing clock time needed to track all particles, as well as to complexities associated with the computational load balancing on parallel machines (Garcia 2009).

Eulerian particle methods have been explored as an alternative to Lagrangian particle tracking (Druzhinin & Elghobashi 1998; Ferry & Balachandar 2001, 2002; Kaufmann *et al.* 2008; Masi & Simonin 2014; Masi *et al.* 2014; de Chaisemartin 2009*b*; Laurent *et al.* 2012; Vié *et al.* 2015). The goal of such methods is to solve the statistics of the disperse phase directly. Inspired by approaches in kinetic theory of gases (Chapman & Cowling 1939), the NDF $f(t, x, v_p)$ is defined as the number of particles per unit volume, with certain velocity, v_p, averaged over many realizations. This NDF satisfies a Population Balance Equation (PBE) (referred to as the Williams-Boltzmann equation in the context of spray Williams (1958))

$$\frac{\partial f}{\partial t} + v_{p,i} \frac{\partial f}{\partial x_i} + \frac{\partial}{\partial v_{p,i}} \left(\frac{u_{g,i} - v_{p,i}}{\tau_p} f \right) = 0. \tag{1.3}$$

Equation 1.3 is the equivalent of Eq. 1.2, but is written in a Eulerian framework. However, to avoid solving the NDF in the full phase space, moment methods have been developed (see for instance, Simonin (1996)), which aim to integrate the PBE over the velocity

space to get equation on moments, i.e., integrals over the velocity space. Let us consider a monodisperse cloud of particles, i.e., the same size for all particles at the same location†. The resulting moment equations will be (Simonin 1996)

$$\frac{\partial C}{\partial t} + \frac{\partial C u_{p,j}}{\partial x_j} = 0, \qquad (1.4a)$$

$$\frac{\partial C u_{p,i}}{\partial t} + \frac{\partial C \left(u_{p,i} u_{p,j} + \sigma_{ij} \right)}{\partial x_j} = C \frac{u_i - u_{p,i}}{\tau_p}, \qquad (1.4b)$$

where $C(t, \mathbf{x})$ is the local number density of the particles, $u_{p,i}(t, \mathbf{x})$ is the mean velocity of the particles at the position $\mathbf{x}$, and $\sigma_{ij}(t, \mathbf{x})$ the covariance matrix of the velocity distribution‡

$$C = \int f(t, \mathbf{x}, \mathbf{v_p}) \mathrm{d}\mathbf{v_p}, \qquad (1.5)$$

$$u_{p,i} = \frac{1}{C} \int v_{p,i} f(t, \mathbf{x}, \mathbf{v_p}) \mathrm{d}\mathbf{v_p}, \qquad (1.6)$$

$$\sigma_{ij} = \frac{1}{C} \int \left(v_{p,i} - u_{p,i} \right) \left(v_{p,j} - u_{p,j} \right) f(t, \mathbf{x}, \mathbf{v_p}) \mathrm{d}\mathbf{v_p}. \qquad (1.7)$$

Equation 1.4b needs a closure for the covariance matrix of the NDF. The two quantities that drive the choice are the particle Stokes number St_k based on the Kolmogorov time scale and the volume fraction (Laurent *et al.* 2012). These two quantities control the broadness and shape of the NDF in the velocity space. The Stokes number indicates the occurrence of Particle Trajectory Crossings, i.e., the possibility of multivalued particle velocity at a given space-time instant. It has been shown that for $\mathrm{St}_k < 1$ a monokinetic assumption is indeed valid (Balachandar & Eaton 2011) i.e., only one velocity can describe the particle field per location in physical space. In this range, the covariance is zero, and Eq. 1.4b is closed without any modeling requirement. As classified by Balachandar (Balachandar 2009), three approaches of increasing complexity exist in this range of Stokes number: (i) Dusty gases (Saffmann 1962; Marble 1970) for which the disperse phase velocity is equal to the gas-phase velocity and the disperse-phase total number density is solved for only; (ii) Equilibrium Eulerian (Ferry & Balachandar 2001, 2002) for which the disperse phase is evaluated as an expansion around the gas-phase velocity and, again, only an equation on the disperse-phase total number density is needed; (iii) Monokinetic approach (Druzhinin & Elghobashi 1998; Laurent & Massot 2001), for which the disperse-phase velocity is solved through an additional momentum equation, as in Eq. 1.4. When $\mathrm{St}_k > 1$, particles have sufficient inertia to leave the high-vorticity regions, and particle trajectory crossings occur (Wells & Stock 1983; de Chaisemartin 2009b; Ijzermans *et al.* 2010), also referred to as the Random Uncorrelated Motion (Février *et al.* 2005; Ijzermans *et al.* 2010). In this case when the volume fraction of particles is sufficiently large to allow for many collisions, the velocity distribution relaxes towards the Maxwellian distribution, following the kinetic theory (Chapman & Cowling 1939). For low volume fractions, assumptions have to be made on the NDF itself (Kinetic-Based Moment Methods, Vié *et al.* (2015); Laurent *et al.* (2012)) or on the moment system

† This assumption may be easily relaxed using Multifluid approaches or moment methods, see Laurent & Massot (2001); Kah *et al.* (2012); Vié *et al.* (2013).

‡ Let us emphasize that Eulerian fields are defined in every location in the phase space, either the spatial position or the velocity, whereas Lagrangian particle tracking is defined in a point-particle sense, that is a sum of Dirac's $\delta-$functions in the phase space.

directly (Algebraic-Closure-Based Moment Methods, Kaufmann *et al.* (2008); Masi & Simonin (2014); Masi *et al.* (2014)).

In this study, we use the Monokinetic Eulerian approach. Hence, we will be limited only to the condition of $St_k < 1$, which is still relevant to a broad range of applications. We then focus on addressing two sources of error under such conditions: the statistical convergence and the numerical resolution.

Concerning the statistical convergence, as the Eulerian approach solves the infinite-realization limit of the Lagrangian system, the effect of the number of particles must be assessed. In this context, we ask: how large a particle system would be, to allow for a Lagrangian system to be accurately represented by a Eulerian model? Moreover, we are considering an infinite number of realizations that can modify the gaseous phase in a different way. Consequently, the gas phase obtained from fully Eulerian simulations is an average over each particle realization of the infinite sample. Is the averaged gas phase equivalent to that of the individual particle realization of the Lagrangian reference simulation?

Concerning the numerical resolution, one of the main problems in the Eulerian approach is the design of numerics, as the disperse phase can exhibit large gradients and vacuum zones. Realizable capturing of these extreme conditions inevitably requires numerical methods with inherent dissipation. Here too we ask how fine should be the Eulerian grid to allow for accurate representation of particles and flow field statistics.

In this paper, we first present the modeling approach and the numerics. Then the test configuration is introduced along with the controlling parameters that drive the physics of the problem. We present results for radiatively heated particle-laden flow subject to gravity and buoyancy effects. In this case, heating of the fluid by the particles can generate and sustain turbulence (Zamansky *et al.* 2014). In other words, the particle field, and specifically particle segregation, is the main driver of turbulence in the long run. We then present an analysis on whether the error in the particle segregation due to the under-resolved Eulerian method would have consequences in the prediction of turbulence itself. The paper concludes with a summary of our general recommendations for simulation of particle-laden flows.

2. Simulation methods

Before describing the results of Eulerian and Lagrangian methods, we briefly explain the computational methods and aspects of the model problem used in this study. Equations are spelled out in dimensionless form.

2.1. *Particulate phase equations*

In the Monokinetic assumption, the Eulerian Moment method equations for the dimensionless concentration C, and velocity $u_{p,i}$ are (Laurent & Massot 2001)

$$\frac{\partial C}{\partial t} + \frac{\partial C u_{p,j}}{\partial x_j} = 0, \tag{2.1}$$

$$\frac{\partial C u_{p,i}}{\partial t} + \frac{\partial C u_{p,i} u_{p,j}}{\partial x_j} = C \frac{u_i - u_{p,i}}{\tau_p}. \tag{2.2}$$

2.2. *Gas phase equations*

The equations for dimensionless gas density ρ, velocity u_i and temperature T are

$$\frac{\partial \rho}{\partial t} + \frac{\partial \rho u_j}{\partial x_j} = 0, \tag{2.3}$$

$$\frac{\partial \rho u_i}{\partial t} + \frac{\partial \rho u_i u_j}{\partial x_j} = -\frac{\partial P}{\partial x_i} + \nu \frac{\partial}{\partial x_j} \left(\frac{\partial u_i}{\partial x_j} + \frac{\partial u_j}{\partial x_i} - \frac{2}{3}\delta_{ij}\frac{\partial u_k}{\partial x_k} \right) + (\rho - 1)\, g_i, \tag{2.4}$$

$$\frac{1}{\gamma}\frac{\partial \rho T}{\partial t} + \frac{\partial \rho T u_j}{\partial x_j} = \frac{\nu}{\text{Pr}} \frac{\partial}{\partial x_i} \left(\frac{\partial T}{\partial x_i} \right) + \alpha(C - 1), \tag{2.5}$$

where ν is the dimensionless viscosity, Pr the Prandtl number, γ the heat capacity ratio, g the dimensionless gravity, and α the radiative heat flux parameter. Density and temperature are linked through the dimensionless equation of state $\rho T = 1$. The term involving $-g_i$ in the momentum equation represents the hydrostatic pressure gradient. Here we have included this term explicitly to allow for use of a periodic assumption in the remaining portion of the pressure field. The term $-\alpha$ in the energy equation stands for a homogeneous cooling in order to avoid global energy accumulation. Therefore, we subtract the mean energy added by the radiative input from the domain.

2.3. *Numerical methods*

These gas phase equations are solved using the low-Mach number approximation (Choi & Merkle 1993; Guillard & Viozat 1998). Spatial derivatives are evaluated through second-order central differences. The variable coefficient Poisson equation for aerodynamic pressure is solved using FFT in an iterative procedure to account for dilatability effects. For time integration of the Eulerian moment methods, a second-order scheme is used (Bouchut *et al.* 2003; de Chaisemartin 2009*a*). Integration of the source terms is performed using a second-order Strang Splitting. The limiter used for slope evaluation is a double minmod (Sabat *et al.* 2014*a*,*b*) to handle the large gradients which the particle concentration and velocity fields are subject to.

In the Lagrangian tracking, a fourth-order Runge-Kutta method is used to solve Eq. 1.2. A second-order linear interpolation is used for gas phase-disperse phase exchanges (Apte *et al.* 2003).

2.4. *Initial conditions and controlling parameters*

In the present work, the domain we consider is a triply periodic box with no mean flow ($< u_i >= 0$). The heat capacity ratio γ is equal to 1.4 and the Prandtl number $\text{Pr} = \frac{c_p \mu}{\lambda}$ is equal to 1.0.

The Reynolds number Re is set by the initial condition of the turbulence. Here we use a Passot-Pouquet spectrum (Passot & Pouquet 1987) with a Reynolds number based on the Taylor microscale $\text{Re}_\lambda = 27$ with a total kinetic energy equal to 3 and a dimensionless viscosity $\nu = 1.46 \times 10^{-3}$. As no artificial forcing is considered, the turbulent energy will decay if no physical forcing is involved.

The radiative heat flux parameter α controls the heating level through particle accumulations in the domain, thus driving the final state of turbulence. This parameter will be fixed at $\alpha = 0.1$. As this parameter is fixed, the next parameter will vary the turbulence level.

The relaxation time of the particles τ_p controls the level of inertia of the particles, and thus their preferential concentration (Eaton & Fessler 1994). This is a key parameter because it will decide whether our Eulerian approach is adapted or not. In the following,

we will consider $\tau_p = 0.01, 0.025, 0.05, 0.10, 0.20, 0.40$, and 0.80. This dimensionless relaxation time is linked to the Stokes number St_k.

Concerning the size of the domain, Zamansky *et al.* (2014) and Yoshimoto & Goto (2007) stated that the ratio between the scales of turbulence and the box size influences the development of turbulence and preferential concentration. In the present study, as our goal is mainly to compare Eulerian and Lagrangian approaches, we will not investigate this issue, but keep the same domain size for every test case, i.e., $L_{box} = 2\pi$. Combining the Reynolds number and the domain size, the nominal mesh size for resolving the turbulence at initial conditions is 64^3 cells.

Finally, particles are uniformly distributed at time $t = 0$: for the Lagrangian particle tracking, they are randomly drawn over the entire space, whereas for the Eulerian simulations, the initial concentration is set to $C(t, \mathbf{x}) = 1$. In terms of the number of particles, as we are interested in the statistical convergence, we investigate cases with 1 and 256 particles per cell, i.e., 0.262M and 67M particles in the whole domain. All simulations start with a particulate phase at rest, i.e., $\mathbf{u}_p(t = 0, \mathbf{x}) = 0$ or $\mathbf{V}_p(t = 0) = 0$.

2.5. *Post-processing*

To analyze each test case, we investigate macroscopic quantities obtained by spatially averaging over the domain $\langle \cdot \rangle$. For the gas phase, we focus on the Turbulent Kinetic Energy (TKE) of the gas phase $\langle u_{g,i}^2 \rangle$ as a measure of the turbulence level, and the temperature variance $\left\langle T_g'^2 \right\rangle = \left\langle T_g^2 \right\rangle - \left\langle T_g \right\rangle^2$, as a measure of the effect of segregation on the heat exchange between the two phases.

For the disperse phase, we investigate two statistical quantities: the Turbulent Kinetic Energy of the particulate phase (PTKE), as a measure of the effect of the turbulence level on the dynamics of the particles, and the segregation of the particulate phase as a measure of preferential concentration effects due to the turbulence.

The disperse phase quantities are evaluated in a different way for each modeling approach. For the Lagrangian particle tracking method, the PTKE is evaluated as the average over all particles

$$\mathrm{PTKE} = \frac{1}{N_p} \sum_{k=1}^{N_p} V_{k,i}^2, \qquad (2.6)$$

whereas in the Eulerian method, PTKE is defined as $\left\langle u_{p,i}^2 \right\rangle$.

Segregation is defined as the normalized mean square concentration. However, given that for the Lagrangian particles, the definition of concentration is scale dependent, a reference projection scale needs to be defined. In Vié *et al.* (2015), the authors used a reference mesh as a projection for mesh for all Lagrangian and Eulerian quantities. Here the native scale is arbitrarily defined as the nominal Kolomogorov-resolved mesh for the initial conditions, that is 64^3 cells. Consequently, we define a projected particle number density as

$$C_{\mathrm{Lag}}(t, \mathbf{x}) = \frac{1}{N_p \delta_E^3} \sum_{k=1}^{N_p} \int \delta(\mathbf{x} - \mathbf{X}_k) \mathcal{H}(\mathbf{x}|\delta_E) \mathrm{d}\mathbf{x}, \qquad (2.7)$$

where $\mathcal{H}$ is the cubic hat function centered at $\mathbf{x}$ and of characteristic width δ_E. In our simulations, δ_E is equal to the reference grid spacing of the Lagrangian simulations, i.e.,

$\delta_E = 2\pi/64$. It follows that the Lagrangian evaluation of the segregation is

$$g_{pp}^{\text{Lag}} = \frac{\left\langle C_{\text{Lag}}^2 \right\rangle}{\left\langle C_{\text{Lag}} \right\rangle^2}. \tag{2.8}$$

For the Eulerian approach, to be consistent with the Lagrangian method, the concentration field is also projected onto the reference mesh of the Lagrangian simulations and then the segregation is evaluated as

$$g_{pp}^{\text{Eul}} = \frac{\left\langle C_{\text{proj}}^2 \right\rangle}{\left\langle C_{\text{proj}} \right\rangle^2}, \tag{2.9}$$

where C_{proj} is the projected concentration field. At this point, we emphasize that even for a statically uniform distribution for the Lagrangian Particle, the segregation is not equal to exactly one. As they are randomly and independently drawn, the local number of particles follows the Poisson distribution. Thus the segregation for a homogeneous Lagrangian sampling can be shown to be $g_{pp} = (\lambda + 1)/\lambda$ where λ is the number of particles per cell. Consequently, the initial segregation of the Lagrangian computations is $g = 2$ and 1.003 for 1 and 256 particles per cell.

In our test case, gravity and radiation are active. As explained by Zamansky *et al.* (2014), a buoyancy-driven turbulence is triggered, resulting in long-term statistically stationary and homogeneous signals. To analyze these signals, the temporal mean of the spatially averaged statistics is investigated.

3. Results

In the following, for each case we first present statistical results from Lagrangian calculations. The most important quantity which is highly sensitive to the number of particles is the segregation. Once impact of statistical convergence for this quantity is established, we present results of the corresponding Eulerian simulations, and demonstrate the resolution requirement to capture each field. Both Lagrangian and Eulerian calculations are performed over a wide range of parameters by varying the particle Stokes number.

3.1. *Statistical convergence*

In Figure 1, the temporal means of the segregation and the PTKE are plotted against the relaxation time of the particles. The number of particles has a great effect on the segregation. For the PTKE, it has a negligible influence for moderate to large relaxation time, while the most significant effect is found for the smallest relaxation time, for which the segregation is mainly due to the lack of statistical convergence. This is similar to temperature statistics in Figure 2), and is expected, given that the induced turbulence is highly influenced by the local gas temperature. This is also consistent with results in Zamansky *et al.* (2014), obtained under the Boussinesq-Oberneck assumption.

Figure 3 shows the mean Kolmogorov time and length scales for different particle relaxation times. This information can be used to determine the range of particle relaxation times for which the long term Stokes number is less than unity, as shown with the intersection with the dashed line. Next we examine Eulerian simulations in this range.

3.2. *Comparison between Lagrangian and Eulerian results*

Finally, the ability of the Eulerian method to reproduce the Lagrangian results is assessed in this test case in which turbulence itself is coupled with particle segregation. In this
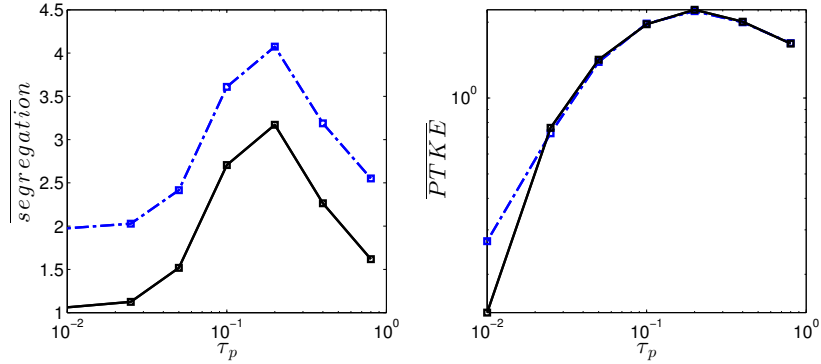
FIGURE 1. Turbulence with radiation and gravity: effect of the number of particles on the statistics of the Lagrangian simulations. Mean segregation (left) and Particle Total Kinetic Energy (right) versus τ_p, for 1 particle per cell (dashed line) and 256 particles per cell (full line).
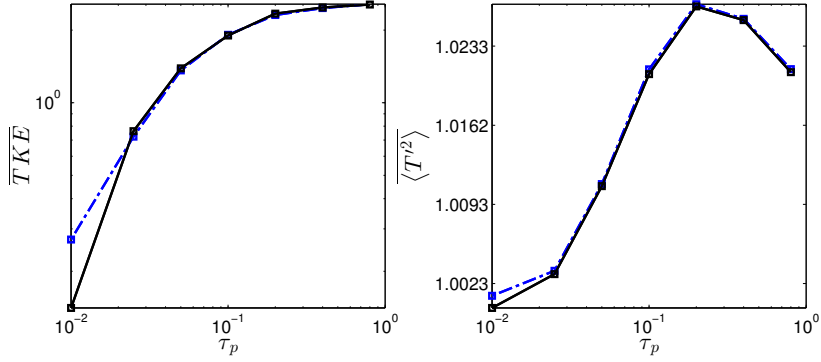

FIGURE 2. Turbulence with radiation and gravity: effect of the number of particles on the statistics of the Lagrangian simulations. Mean Total Kinetic Energy (left) and Temperature variance (right) versus τ_p, for 1 particle per cell (dashed line) and 256 particles per cell (full line).
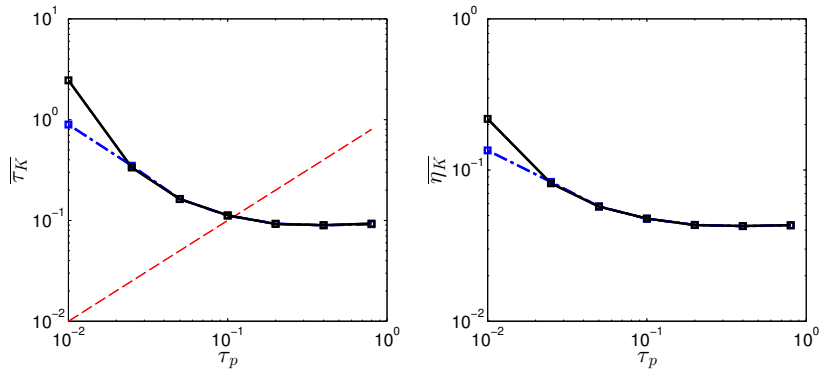

FIGURE 3. Turbulence with radiation and gravity: effect of the number of particles on the statistics of the Lagrangian simulations. Mean Kolmogorov time (left) and length (right) scales versus τ_p, for 1 particle per cell (dot-dashed line) and 256 particles per cell (full line). The dashed line corresponds to a Stokes number based on the Kolmogorov time scale equal to one.
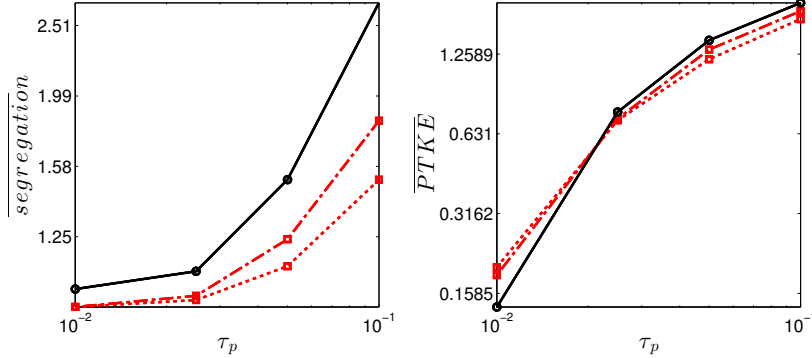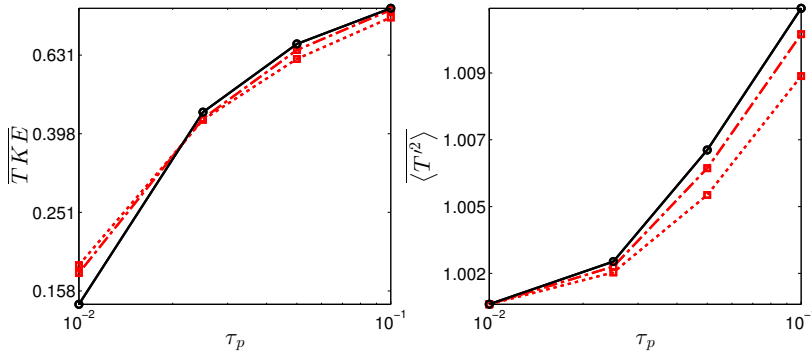
FIGURE 4. Turbulence with radiation and gravity: Lagrangian (black) versus Eulerian (red) simulations with 64^3 (dotted line) and 128^3 (dot-dashed line) cells. Mean segregation (left) and Particle Total Kinetic Energy (right) versus τ_p.

FIGURE 5. Turbulence with radiation and gravity: Lagrangian (black) versus Eulerian (red) simulations with 64^3 (dotted line) and 128^3 (dot-dashed line) cells. Mean Total Kinetic Energy (left) and temperature variance (right) versus τ_p.

test case, the temperature field generated by the heat transfer from the disperse phase to the gas triggers turbulence through buoyancy effects. The question is whether the unresolved temperature field will influence the statistics of the generated turbulence.

Our simulations confirmed that the employed Eulerian method can reach a self-sustained turbulence, which is the minimal requirement for assessing the validity of the Eulerian strategy. Temporally averaged quantities are compared in Figures 4-5. The segregation is underestimated, whereas the PTKE is relatively well predicted. A similar conclusion is reached for the gas-phase TKE, and temperature variance. Finally, the Kolmogorov scales of the generated flows are evaluated in Figure 6. Results shows a good agreement between Lagrangian and Eulerian results. Moreover, we confirm that simulation with relaxation time below 0.1 corresponds to a Stokes number below one, thus justifying the validity of the present Monokinetic closure.

4. Conclusion

In the present work, Eulerian and Lagrangian strategies to describe a thermally two-way coupled system have been compared. In the configuration introduced in Zamansky *et al.* (2014), a self-sustained turbulence is generated by the thermal coupling between
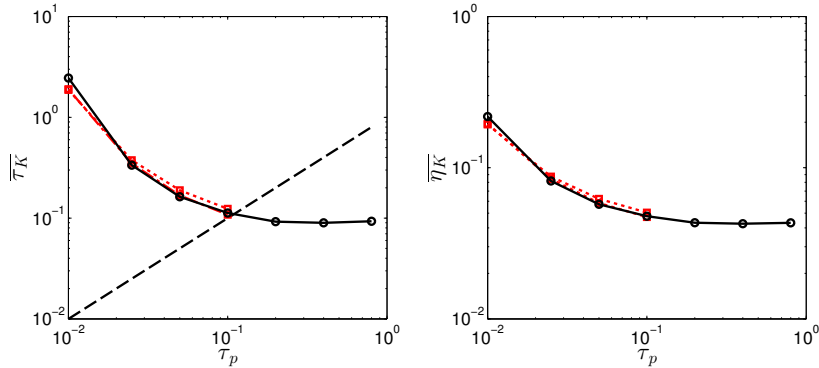
FIGURE 6. Turbulence with radiation and gravity: Lagrangian (black) versus Eulerian (red) simulations with 64^3 (dotted line) and 128^3 (dot-dashed line) cells. Kolmogorov time (left) and length (right) scales versus τ_p. The dashed line corresponds to a Stokes number based on the Kolmogorov time scale equal to one.

a disperse phase subject to a homogeneous radiation input and a gas phase subject to buoyancy effects. The generated feedback loop is a preferred benchmark to assess the ability of Eulerian methods to reproduce the physics of a two-way coupled system.

As the Eulerian methods solve the statistics of the disperse phase over an infinite number of realizations whereas the reference Lagrangian particle tracking solves an individual realization, the effect of the number of particles, and thus statistical convergence, has first been assessed for Lagrangian simulations. Results demonstrated the important effect of the number of particles on the segregation statistics of the disperse phase, as expected. However, it turned out these discrepancies do not affect the gas statistics, as they are weakly sensitive to the number of particles. Another interesting conclusion is the fact that the gas phase obtained from both methods is equivalent, even if the Eulerian method is intrinsically averaging the gas phase over an infinite sample of particle realization.

The Eulerian approach that has been chosen is the Monokinetic moment method. As it cannot capture more than one velocity per position, this strategy is valid only if no particle trajectory crossing occurs, thus limiting the range of interest of our comparisons to a Stokes number based on the Kolmogorov time scale below one. For the sake of comparison, a statistically converged Lagrangian solution has been selected as a reference. Results have demonstrated the ability of the method to reproduce the gas phase statistics accurately, whereas the segregation of the disperse phase is still challenging to capture because of numerical diffusion effects. We also mentioned that this numerical diffusion has no effect on the gas phase statistics, as the thermal diffusion of the gas phase makes the gas temperature field less sensitive to disperse phase structures smaller than the diffusive scale.

In conclusion, as long as the evolution of the flow is not determined by individual particle effects, the Monokinetic Eulerian moment method is an accurate way to describe gas-particle flows in a two-way context, as long as no significant particle trajectory crossing occurs. In the case of very small Stokes numbers, where results are highly sensitive to the number of particles involved, Lagrangian simulations are still the preferred method, and new developments are necessary for Eulerian methods. As a perspective, it is envisioned that high-order moment methods (Vié *et al.* 2015; Laurent *et al.* 2012), would be able to reproduce particle trajectory crossings. High-order numerical methods could

also be used, like Discontinous Galerkin approaches (Sabat *et al.* 2014*b,a*), to reduce the mesh requirements of the Eulerian simulations as well as the CFL number sensitivity highlighted for the case with radiation and no gravity.

5. Acknowledgments

REFERENCES

Apte, S. V., Mahesh, K., Moin, P. & Oefelein, J. C. 2003 Large-eddy simulation of swirling particle-laden flows in a coaxial-jet combustor. *Int. J. Multiphase Flow* **29**, 1311–1331.

Balachandar, S. 2009 A scaling analysis for point-particle approaches to turbulent multiphase flows. *Int. J. Multiphase Flow* **35**, 801–810.

Balachandar, S. & Eaton, J. 2011 Turbulent dispersed multiphase flow. *Ann. Rev. Fluid Mech.* **42**, 111–133.

Boivin, M., Simonin, O. & Squires, K. 1998 Direct numerical simulation of turbulence modulation by particles in isotropic simulation. *J. Fluid Mech.* **375**, 235–263.

Bouchut, F., Jin, S. & Li, X. 2003 Numerical approximations of pressureless and isothermal gas dynamics. *SIAM J. Num. Anal.* **41**, 135–158.

de Chaisemartin, S. 2009*a* Eulerian models and numerical simulation of turbulent dispersion for polydisperse evaporating sprays. PhD thesis, Ecole Centrale Paris, France, available online at http://tel.archives-ouvertes.fr/tel-00443982/en/.

de Chaisemartin, S. 2009*b* Eulerian models and numerical simulation of turbulent dispersion for polydisperse evaporation sprays. PhD thesis, Ecole Centrale Paris, France, available on TEL : http://tel.archives-ouvertes.fr/tel-00443982/en/.

Chapman, S. & Cowling, T. 1939 *The mathematical theory of non-uniform gazes*. Cambridge University Press.

Choi, Y. H. & Merkle, C. L. 1993 The application of preconditioning in viscous flows. *J. Comput. Phys.* **105**, 207–230.

Druzhinin, O. & Elghobashi, S. 1998 Direct numerical simulations of bubble-laden turbulent flows using the two-fluid formulation. *Phys. Fluids* **10**, 685–697.

Eaton, J. K. & Fessler, J. R. 1994 Preferential concentration of particles by turbulence. *Int. J. Multiphase Flow* **20**, 169–209.

Elgobashi, S. & Truesdell, G. 1992 Direct simulation of particle dispersion in a decaying isotropic turbulence. *J. Fluid Mech.* **242**, 655–700.

Elgobashi, S. & Truesdell, G. 1993 On the two-way interaction between homogeneous turbulence and dispersed solid particles. *Phys. Fluids* **5**, 1790–1801.

Ferry, J. & Balachandar, S. 2001 A fast Eulerian method for disperse two-phase flow. *Int. J. Multiphase Flow* **27**, 1199–1226.

Ferry, J. & Balachandar, S. 2002 Equilibrium expansion for the eulerian velocity of small particles. *Powder Technology* **125**, 131–139.

Fessler, J. R., Kulick, J. D. & Eaton, J. K. 1994 Preferential concentration of heavy particles in a turbulent channel flow. *Phys. Fluids* **6**, 3742–3749.

Février, P., Simonin, O. & Squires, K. D. 2005 Partitioning of particle velocities in gas-solid turbulent flow into a continuous field and a spatially uncorrelated random distribution: theoretical formalism and numerical study. *J. Fluid Mech.* **533**, 1–46.

Fox, R. O. 2012 Large-Eddy-Simulation tools for multiphase flows. *Ann. Rev. Fluid Mech.* **44**, 47–76.

Garcia, M. 2009 *Development and validation of the Euler-Lagrange formulation on a parallel and unstructured solver for large-eddy simulation.* Ph.D. Thesis, Université Toulouse III, France.

Gore, R. A. & Crowe, C. T. 1989 The effect of particle size on modulating turbulent intensity. *Int. J. Multiphase Flow* **15**, 279–285.

Guillard, H. & Viozat, C. 1998 On the behaviour of upwind schemes in the low mach number limit. *Comput. Fluids* **28**, 63–86.

Ijzermans, R. H. A., Meneguz, E. & Reeks, M. W. 2010 Segregation of particles in incompressible random flows: singularities, intermittency and random uncorrelated motion. *J. Fluid Mech.* **653**, 99–136.

Kah, D., Laurent, F., Massot, M. & Jay, S. 2012 A high order moment method simulating evaporation and advection of a polydisperse spray. *J. Comput. Phys.* **231**, 394–422.

Kaufmann, A., Moreau, M., Simonin, O. & Helie, J. 2008 Comparison between Lagrangian and mesoscopic Eulerian modelling approaches for inertial particles suspended in decaying isotropic turbulence. *J. Comput. Phys.* **227**, 6448–6472.

Laurent, F. & Massot, M. 2001 Multi-fluid modeling of laminar poly-dispersed spray flames: origin, assumptions and comparison of the sectional and sampling methods. *Combust. Theor. Model.* **5**, 537–572.

Laurent, F., Vié, A., Chalons, C., Fox, R. O. & Massot, M. 2012 A hierarchy of Eulerian models for trajectory crossing in particle-laden turbulent flows over a wide range of Stokes numbers. *Annual Research Briefs,* Center for Turbulence Research, Stanford University, pp. 193–204.

Marble, F. 1970 Dynamics of dusty gases. *Ann. Rev. Fluid Mech.* **2**, 397–446.

Masi, E. & Simonin 2014 Algebraic-closure-based moment method for unsteady eulerian simulations of non-isothermal particle-laden turbulent flows at moderate stokes numbers in dilute regime. *Flow Turbul. Combus.* **92**, 121–145.

Masi, E., Simonin, O., Riber, E., Sierra, P. & Gicquel, L. 2014 Development of an algebraic-closure-based moment method for unsteady eulerian simulations of particle-laden turbulent flows in very dilute regime. *Int. J. Multiphase Flow* **58**, 257–278.

Maxey, M. & Riley, J. 1983 Equation of motion for a small rigid sphere in a non uniform flow. *Phys. Fluids* **26**, 2883–2889.

Mizukami, M., Parthasarathy, R. N. & Faeth, G. M. 1992 Particle-generated turbulence in homogeneous dilute dispersed flows. *Int. J. Multiphase Flow* **18**, 397–412.

Passot, T. & Pouquet, A. 1987 Numerical simulation of compressible homogeneous flows in turbulent regime. *J. Fluid Mech.* **181**, 441–466.

Riley, J. J. & Patterson, G. S. 1974 Diffusion experiments with numerically intergrated isotropic turbulence. *Phys. Fluids* **17**, 292–297.

Sabat, M., Larat, A., Vié, A. & Massot, M. 2014a Comparison of realizable

schemes for the eulerian simulation of disperse phase flows. *FVCA7, Springer proceedings in Mathematics and Statistics* **78**, 935–943.

SABAT, M., LARAT, A., VIÉ, A. & MASSOT, M. 2014*b* On the development of high order realizable schemes for the Eulerian simulation of disperse phase flows: a convex-state preserving Discontinuous Galerkin method. *J. Comput. Multiphase Flows* **6**, 247–270.

SAFFMANN, U. 1962 On the stability of laminar flow of a dusty gas. *J. Fluid Mech.* **13(1)**, 120–128.

SIMONIN, O. 1996 *Combustion and turbulence in two phase flows.* Lecture series 1996-02.

SQUIRES, K. & EATON, J. 1991*a* Measurements of particle dispersion obtained from direct numerical simulations of isotropic turbulence. *J. Fluids Mech.* **226**, 1–35.

SQUIRES, K. D. & EATON, J. 1991*b* Preferential concentration of particles by turbulence. *Phys. Fluids* **3**, 1169–1178.

STOKES, G. 1851 On the effect of the inertial friction of fluids on the motions of pendulums. *Trans. Cambridge Phil. Soc.* **9**.

SUNDARAM, S. & COLLINS, L. R. 1997 Collision statistics in an isotropic particle-laden turbulent suspension. part 1. direct numerical simulations. *J. Fluid Mech.* **335**, 75–109.

VIÉ, A., DOISNEAU, F. & MASSOT, M. 2015 On the Anisotropic Gaussian closure for the prediction of inertial-particle laden flows. *Commun. Comput. Phys.* **17** (1), 1–46.

VIÉ, A., LAURENT, F. & MASSOT, M. 2013 Size-velocity correlations in hybrid high order moment/multi-fluid methods for polydisperse evaporating sprays: modeling and numerical issues. *J. Comput. Phys.* **237**, 177–210.

WANG, L. P., WEXLER, A. S. & ZHOU, Y. 1998 On the collision rate of small particles in isotropic turbulence, ii finite inertia case. *Phys. Fluids* **10** (10), 1206–1216.

WELLS, M. R. & STOCK, D. E. 1983 The effects of crossing trajectories on the dispersion of particles in a turbulent flow. *J. Fluid Mech.* **136**, 31–62.

WILLIAMS, F. A. 1958 Spray combustion and atomization. *Phys. Fluids* **1**, 541–545.

YOSHIMOTO, H. & GOTO, S. 2007 Self-similar clustring of inertial particles in homogeneous turbulence. *J. Fluid Mech.* **577**, 275–286.

ZAMANSKY, R., COLETTI, F., MASSOT, M. & MANI, A. 2014 Radiation induces turbulence in particle-laden fluids. *Phys. Fluids* **26**, 071701.